



Shielding effectiveness adjustment of planar mesh screen by fine-tuning metal thickness

Yonathan Corredores, Xavier Castel, Philippe Besnier, Cyril Dupeyrat,
Patrice Foutrel

► To cite this version:

Yonathan Corredores, Xavier Castel, Philippe Besnier, Cyril Dupeyrat, Patrice Foutrel. Shielding effectiveness adjustment of planar mesh screen by fine-tuning metal thickness. The Journal of Engineering, 2018, 2018 (4), pp.239-241. 10.1049/joe.2018.0070 . hal-01715650

HAL Id: hal-01715650

<https://hal.science/hal-01715650>

Submitted on 12 Jul 2019

HAL is a multi-disciplinary open access archive for the deposit and dissemination of scientific research documents, whether they are published or not. The documents may come from teaching and research institutions in France or abroad, or from public or private research centers.

L'archive ouverte pluridisciplinaire **HAL**, est destinée au dépôt et à la diffusion de documents scientifiques de niveau recherche, publiés ou non, émanant des établissements d'enseignement et de recherche français ou étrangers, des laboratoires publics ou privés.



Distributed under a Creative Commons Attribution - NonCommercial 4.0 International License

SE adjustment of planar mesh screen by fine-tuning metal thickness

Yonathan Corredores¹, Xavier Castel¹, Philippe Besnier¹, Cyril Dupeyrat², Patrice Foutrel²

¹Institut d'Electronique et de Télécommunications de Rennes, IETR UMR-6164, IUT de Saint-Brieuc/Université de Rennes 1, 18 rue Henri Wallon, 22004 SAINT-BRIEUC; & INSA de Rennes, 20 avenue des Buttes de Coësmes, 35708 Rennes, France

²SAFRAN Electronics & Défense, SAFRAN Group, 21 avenue du Gros Chêne, 95610 Eragny, France

E-mail: xavier.castel@univ-rennes1.fr

Published in *The Journal of Engineering*; Received on 16th January 2018; Revised on 6th February 2018; Accepted on 8th February 2018

Abstract: The study presents the thickness effect of mesh metal films printed onto glass substrate on the shielding effectiveness (SE) of such transparent screens. Currently, standards in microelectronic technology use a metal film thickness of between ~ 100 nm and few micrometres, depending on the available deposition and implementation techniques. This study demonstrates that the thickness of mesh metal films is a key parameter which needs to be adjusted precisely. A theoretical model based on SE, complex impedance and optical transparency has been developed for this purpose. At microwaves, a relevant selection of the metal thickness values from 0.1 to 2 μm changes the SE at low frequency (from 36 to 40 dB at 2 GHz, respectively) while maintaining it constantly at a higher frequency (close to 20 dB at 18 GHz). The optical transparency of such mesh screens is kept constant over the entire visible light spectrum (78%). Experimental data are in complete agreement with the theoretical values.

1 Introduction

Electromagnetic interference (EMI) has become a significant problem for various electronic applications. In consequence, the design of robust protection against EMI is nowadays an important issue, particularly for telecommunication and radar environments. Such applications on glazing or screens require high optical transparency over the entire visible light spectrum in addition. Thin film technology offers an appropriate response to these constraints [1]. Currently, mesh metal film solution is used not only for its available electromagnetic protection, but also for its high optical transmission [2]. Both depend on the mesh parameters, namely the pitch and the metal strip width. Standards in microelectronic technology use a metal film thickness within a range from ~ 100 nm to few micrometres [3], depending on the available deposition and implementation techniques. The aim of the present work is to demonstrate that the thickness of the mesh metal film is also a key parameter that is not exclusively dependent on technology requirements. Indeed, the mesh metal thickness must be precisely adjusted when setting up the design of the proposed EMI protection. For this, a theoretical model based on shielding effectiveness (SE), complex impedance and optical transparency has been developed and briefly detailed in the second section of this paper. The impact of the mesh metal film thickness on the above theoretical values is investigated. The fabrication process of such mesh metal films is described in the third section of this paper. Experimental results are then presented, compared and discussed. Finally, the conclusion is drawn.

2 Theoretical model and numerical values

Use of metal meshes as electromagnetic filters has been initially proposed by Ulrich in 1967 [4]. Afterwards, several works have been published improving the existing model [3, 5]. The theoretical model developed here is based on the well known transmission line approach taking into account the complex impedances Z_c of the mesh metal structure, Z_s of the substrate and Z_0 of the air, as detailed in [6]. The metal impedance Z_c is computed from (1) derived in [6], depending on the thickness t_f of the mesh metal

film, as follows:

$$Z_c = \frac{(1+j)}{\sigma_f \delta_f \tanh\left((1+j)(t_f/\delta_f)\right)} \times \frac{g}{2a} + Z_0 \frac{g}{\lambda_0} \ln\left(\frac{1}{\sin((\pi a/g))}\right)j = R + jX \quad (1)$$

where σ_f is the conductivity of the metal, δ_f is the skin depth at the operating frequency, g is the mesh pitch, $2a$ is the metal strip width of the mesh, λ_0 is the wavelength at the operating frequency, R is the resistance and X is the reactance of the mesh structure.

SE is computed from the modulus of the total transmission scattering parameter S_{21}^T in (2) between two transmission lines separated by the mesh metal film/substrate interface, as follows:

$$SE = 20 \times \log_{10}(|S_{21}^T|) \quad (2)$$

The cross-sectional and top views of the square mesh structure printed onto glass substrate are depicted in Fig. 1. Optical transparency (T_O) of such samples is deduced from the ratio between the non-metallised area and the total area, as specified in (3). It is worth noting that T_O is independent of the mesh metal thickness t_f

$$T_O = \frac{(g-2a)^2}{(g)^2} \times (1-R_1)^2 \quad (3)$$

where R_1 is the light reflection coefficient of the bare glass surface. Glass absorbance is neglected here.

A silver mesh ($\sigma_f = 6.1 \times 10^7$ S/m; $2a = 30 \mu\text{m}$; $g = 347 \mu\text{m}$) has been designed on lossless glass substrate ($t_s = 0.7$ mm; $R_1 = 0.04$; $\varepsilon_r = 5$). Values of the parameters ($2a$; g) have been specifically selected here because (i) they provide a theoretical optical transparency of the mesh screen close to 80% (Table 1) and (ii) they are easy to achieve using standard microelectronic technology (as described in the following section). The computed optical

transparency value includes the Fresnel loss of the glass substrate [4% for each side, R_1 in (3)]. Therefore, the transparency of the bare glass substrate is equal to 92%. Four different mesh thicknesses have been set here: 0.1, 0.2, 0.5 and 2 μm . The computed sheet resistance R_s is equal to the real part R of Z_c in DC mode [see (1)]. As expected, R_s values depend on the mesh metal thickness t_f (Table 1). On the one hand, at high frequency (18 GHz), SE is equal to 20 dB regardless of the thickness of the mesh silver films (Fig. 2). On the other hand, at low frequency (below 6 GHz), SE depends on the silver film thickness. At 2 GHz, SE is the same (40 dB) for the 2 and 0.5 μm thick mesh silver films. For the 0.2 μm thick mesh film, SE is minimally weaker (39 dB). Moreover, for the thinnest mesh film (0.1 μm thick), a significant reduction of SE is highlighted (36 dB, Fig. 2).

The shape of SE curves (Fig. 2) depends on the relative variation of the resistance R and the reactance X of the mesh metal structure impedance Z_c in (1). R -value depends on the metal thickness and is independent of the mesh pattern ($2a$; g) by contrast with X which depends on the mesh pattern ($2a$; g) and is independent of the metal thickness. At high frequency, SE is monitored by reactance X ($X \gg R$). As an identical mesh pattern is used in the present work, the four curves overlap perfectly. At low frequency, SE is monitored by resistance R and reactance X , which exhibit both the same order of magnitude (with $X \geq R$). As R -value depends on the metal thickness, the greater the thickness t_f is, the better the SE will be, up to the limit of $t_f \approx \delta_f$ ($\delta_f = 1.4 \mu\text{m}$ at 2 GHz). Beyond that limit, the metal thickness is no longer contributing to SE of such mesh screens.

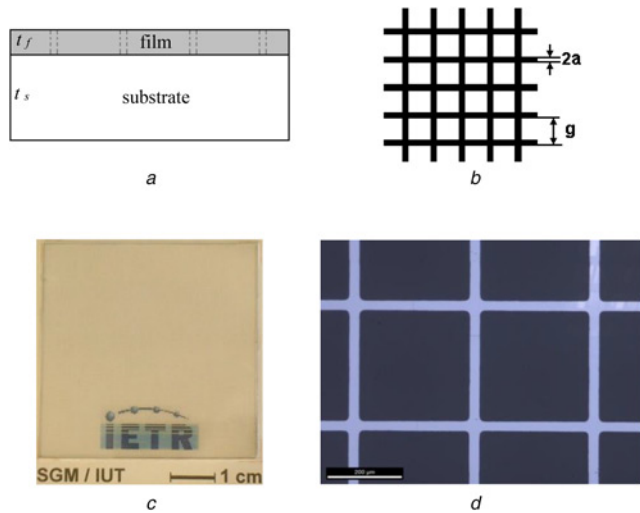


Fig. 1 Mesh metal film (thickness t_f) printed onto glass substrate (thickness t_s)

- a Cross-sectional view
- b Top view with metal strip width $2a$ and pitch g of the mesh structure
- c Picture of a mesh silver/titanium film ($t_f = 2 \mu\text{m}$) placed above the Institute logo
- d Detail of a mesh silver/titanium film ($t_f = 2 \mu\text{m}$) with $2a = 30 \mu\text{m}$ and $g = 347 \mu\text{m}$ (optical microscopy picture)

Table 1 Comparison of the theoretical and measured values of optical transparency T_O (at $\lambda_0 = 550 \text{ nm}$) and sheet resistance R_s of the mesh silver films according to different metal thicknesses t_f

thickness $t_f, \mu\text{m}$	0.1	0.2	0.5	2
theoretical $T_O, \%$	78.1	78.1	78.1	78.1
measured $T_O, \%$	77.9	76.9	76.9	78.0
theoretical $R_s, \Omega/\text{sq}$	2.15	1.00	0.43	0.13
measured $R_s, \Omega/\text{sq}$	3.15	1.22	0.48	0.12

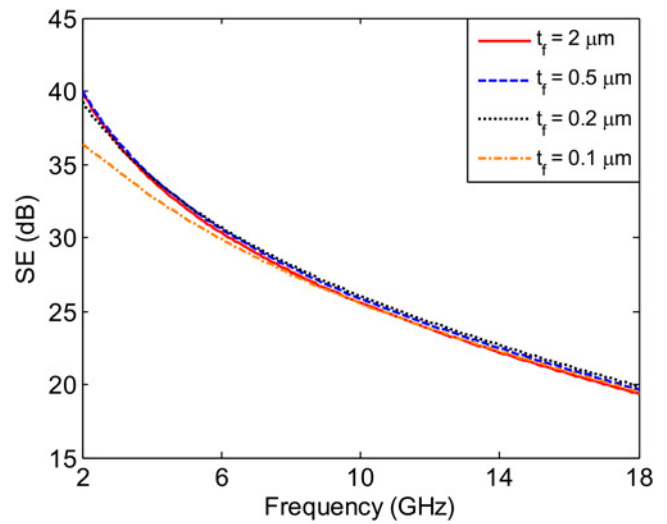


Fig. 2 Theoretical SE of the mesh silver films ($2a = 30 \mu\text{m}$, $g = 347 \mu\text{m}$) according to different metal thicknesses t_f

3 Experiments and measured values

Silver films (t_f thick) and a titanium film (5 nm thick) are both deposited on soda-lime float glass substrates ($50 \text{ mm} \times 50 \text{ mm} \times 0.7 \text{ mm}$) by radio-frequency (RF) magnetron sputtering technique at room temperature. Titanium underlayer is used here only to ensure the strong adhesion of the silver overlayer onto the glass substrate. An RF power density of 2.5 W/cm^2 is used on each working target; argon working pressure is 1.45 Pa and deposition time is adjusted in accordance with the metal thickness as targeted. The sputtering rate has been calibrated for each target (silver: 146 nm/min and titanium: 20 nm/min). Subsequently, a standard photolithographic wet etching process is used to fabricate the mesh silver pattern. First, the samples are spin coated with a photosensitive resin. Then, they are exposed to ultraviolet (UV) light through a photomask with the appropriate pattern. Once the exposed photoresist is developed, the silver and titanium films are successively engraved in suitable chemical solutions. Stripping of the photoresist leaves a periodic array of square apertures in the metal coatings (Figs. 1c and d).

Optical transparency T_O of each sample is recorded at normal incidence by a UV-visible spectrophotometer in the spectral range from 200 to 1100 nm including the Fresnel loss of the glass substrate. Sheet resistance R_s is provided by a standard four-probe setup. The thin film thickness is checked by stylus profilometry. SE of such samples is measured with a Faraday cage placed inside a reverberation chamber according to the nested reverberation chamber procedure, as detailed in [6]. It is worth noting that the SE of a mesh sample with a constant metal thickness (1 μm thick) has already been measured in [6]. Nonetheless, the impact of such metal thickness on the SE response was not investigated as a solution to maintain an identical SE in the upper part of the frequency band while controlling its level in the lower part of the frequency band.

Measured optical transparencies match the predicted one (Fig. 3 and Table 1). Although the same photomask has been used for the fabrication of the four samples, the slight variation in the measured optical transparencies is due to the over-etching during the wet etching step. Measured sheet resistances are also in good agreement with the numerical ones (Table 1). However, departure from theory is observable for the two thinner samples. In the case of ultrathin metal films ($t_f \approx 0.2 \mu\text{m}$ and lower), the specular electron scattering on air/film and film/substrate interfaces restrict the mean free path of conduction electrons. This decreases the experimental conductivity σ_f and explains the relative increase of the measured sheet resistance values.

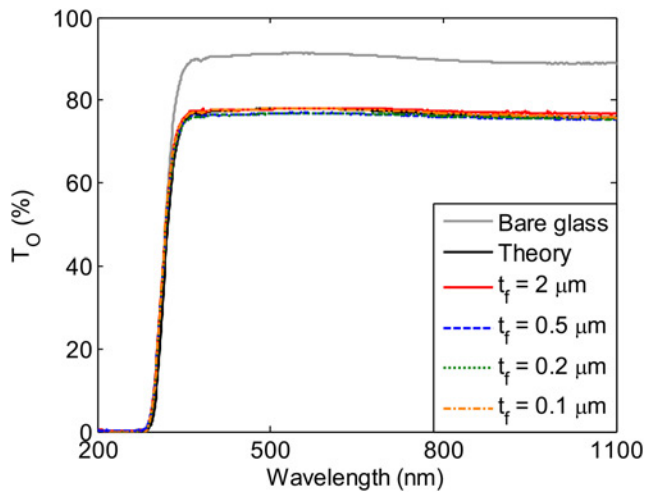


Fig. 3 Theoretical and measured optical transparencies of the mesh silver films ($2a = 30 \mu\text{m}$, $g = 347 \mu\text{m}$) according to different silver thicknesses t_f . Spectrum of the bare glass substrate is also plotted for comparison

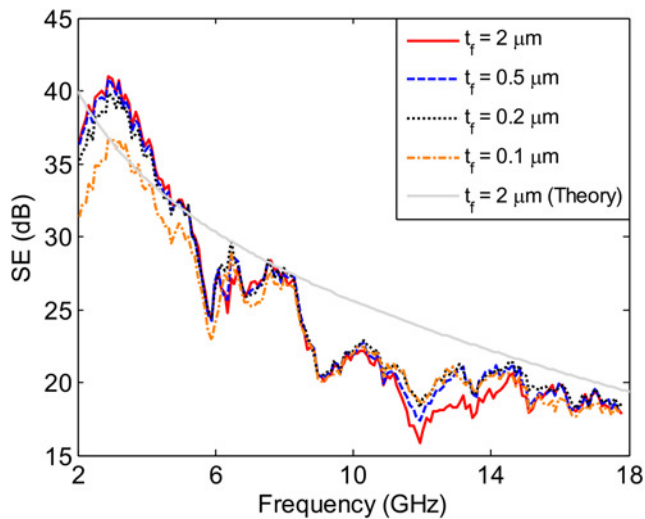


Fig. 4 Measured SE of the mesh silver films ($2a = 30 \mu\text{m}$, $g = 347 \mu\text{m}$) according to different silver thicknesses t_f . Theoretical SE of the $2 \mu\text{m}$ thick mesh silver film is also plotted for comparison

As predicted by the model, measured SE (Fig. 4) at 18 GHz is identical ($\text{SE} = 18.5 \text{ dB}$) regardless of the metal thickness t_f and agrees with the numerical value ($\text{SE} = 20 \text{ dB}$). At low frequency, SE remains also the same for the two samples with $t_f = 0.5$ and $2 \mu\text{m}$ ($\text{SE} = 36 \text{ dB}$ at 2 GHz). Sample with $t_f = 0.2 \mu\text{m}$ exhibits

$\text{SE} = 35 \text{ dB}$ at 2 GHz . Moreover, the thinnest sample ($t_f = 0.1 \mu\text{m}$) presents a significant reduction in its SE ($\text{SE} = 31 \text{ dB}$ at 2 GHz) in accordance with the theoretical model. An SE difference of 5 dB is, therefore, measured between the thickest and thinnest samples, in agreement with theory ($\Delta\text{SE} = 4 \text{ dB}$). It should be noted the presence of amplitude oscillations in Fig. 4 close to 6, 9 and 12 GHz due to the finite size effect of samples, supposed to be an infinite 2D ones within the theoretical model.

4 Conclusion

On the basis of a transmission line model, this paper demonstrates numerically and experimentally that SE of mesh metal films can be adjusted at low frequency by simply selecting the suitable metal thickness. At the same time, optical transparency and SE at a high frequency of such samples are retained. Deposition of the suitable metal thickness makes substantial savings in terms of time and materials, especially when the metal used is semi-precious such as silver. This also allows the use of a single photomask for various available SE of mesh screens at low frequency.

5 Acknowledgments

This work was supported by the European Union through the European Regional Development Fund (ERDF), the Ministry of Higher Education and Research, the Région Bretagne, the Département des Côtes d'Armor and Saint-Brieuc Armor Agglomération, through the CPER Projects 2015-2020 MATECOM and SOPHIE/STIC & Ondes.

6 References

- [1] Hecht D.S., Hu L., Irvin G.: 'Emerging transparent electrodes based on thin films of carbon nanotubes, graphene, and metallic nanostructures', *Adv. Mater.*, 2011, **23**, (13), pp. 1482–1513, doi: 10.1002/adma.201003188
- [2] Lu Z., Wang H., Tan J., *ET AL.*: 'Microwave shielding enhancement of high-transparency, double-layer, submillimeter period metallic mesh', *Appl. Phys. Lett.*, 2014, **105**, p. 241904, doi: 10.1063/1.4904466
- [3] Liu Y., Tan J.: 'Frequency dependent model of sheet resistance and effect analysis on shielding effectiveness of transparent conductive mesh coatings', *Prog. Electromagn. Res.*, 2013, **140**, pp. 353–368, doi: 10.2528/PIER13050312
- [4] Ulrich R.: 'Far-infrared properties of metallic mesh and its complementary structure', *Infrared Phys.*, 1967, **7**, (1), pp. 37–55, doi: 10.1016/0020-0891(67)90028-0
- [5] Whitbourn L.B., Compton R.C.: 'Equivalent-circuit formulas for metal grid reflectors at a dielectric boundary', *Appl. Opt.*, 1985, **24**, (2), pp. 217–220, doi: 10.1364/AO.24.000217
- [6] Corredores Y., Besnier P., Castel X., *ET AL.*: 'Adjustment of shielding effectiveness, optical transmission and sheet resistance of conducting films deposited on glass substrates', *IEEE Trans. Electromagn. Compat.*, 2017, **59**, (4), pp. 1070–1078, doi: 10.1109/TEMC.2017.2654269